https://doi.org/10.5194/egusphere-2026-3738
Preprint. Discussion started: 24 July 2026

Isolating the boreal winter response to the Pinatubo and Krakatoa eruptions using large-ensemble single-forcing simulations

Chaim I. Garfinkel[1], David Avisar[1,2], Wenjuan Huo[3], Ales Kuchar[4], Shoshiro Minobe[5], Scott Osprey[6], Katharina Perny[4], and Jonathon S. Wright[7]

[1]Fredy & Nadine Herrmann Institute of Earth Sciences, The Hebrew University of Jerusalem, Israel
[2]Department of Applied Mathematics, Israel Institute for Biological Research, Ness Ziona, Israel
[3]GEOMAR Helmholtz Centre for Ocean Research Kiel
[4]Institute of Meteorology and Climatology, BOKU University, Vienna, Austria
[5]Department of Earth and Planetary Sciences, Hokkaido University, Sapporo, Japan
[6]Department of Physics, University of Oxford, Oxford, UK
[7]Department of Earth System Science, Institute for Global Change Studies, Ministry of Education Key Laboratory for Earth System Modeling, Tsinghua University, Beijing, China

Correspondence: Chaim Garfinkel (chaim.garfinkel@mail.huji.ac.il)

Abstract. The Northern Hemisphere wintertime circulation response to the eruptions of Krakatoa and Pinatubo is revisited in large ensembles from eight modeling centers with only one time-varying external forcing: volcanic eruptions. All eight models show a warming of the tropical lower stratosphere. In six of the models, the meridional temperature gradient in the winter stratosphere is enhanced, leading to a strengthened stratospheric polar vortex, a positive phase of the North Atlantic Oscillation, a poleward shift in storm tracks, and warm surface temperatures during the winter over subpolar Eurasia. While this warming over subpolar Eurasia is statistically significant in the multi-model mean and in four of the individual models, at least 34 eruptions are needed before it can be robustly distinguished from the global mean cooling with 5% confidence. An El Niño response is evident shortly after eruption in these models, which transitions from a Central Pacific morphology in the first winter to an East Pacific morphology in the second, and subsequently to an La Niña response in the third and fourth winters. While these ENSO responses require 48 or more eruptions to emerge from the noise, they nonetheless lead to surface impacts over North America. However, these surface impacts do not resemble those classically associated with ENSO in the first year after eruption, likely because the tropical precipitation response differs as well due to the large-scale reduction in tropical precipitation. There is substantial diversity in the magnitude of these responses across models, likely owing to differences in tropical stratospheric diabatic heating despite the models using the same forcing.

Plain Language Summary

Whether tropical volcanic eruptions lead to a circulation response in winter is still unclear. We re-evaluate this effect using large ensembles from eight separate models with only one time-varying external forcing: volcanic aerosols. We find that 75% of models simulate the previously proposed effect, but that the signal requires at least 30 eruptions before it emerges robustly from the noise. Furthermore, we demonstrate that the El Nino signal differs from natural El Nino events.

https://doi.org/10.5194/egusphere-2026-3738
Preprint. Discussion started: 24 July 2026

1 Introduction

Shortly after the eruption of Mount Pinatubo in June 1991, several studies proposed that volcanic eruptions can produce surface warming over the Eurasian continent during boreal winter and supported this idea using both observational evidence (e.g., Robock and Mao, 1992, 1995) and modeling results (e.g., Graft et al., 1993; Kirchner et al., 1999). Although this may seem counterintuitive — since volcanic aerosols reduce incoming solar radiation and are typically expected to cause cooling — the idea gained a wide influence because it was supported by a plausible physical explanation, referred to as the "stratospheric pathway" (Graft et al., 1993; Kodera, 1994).

In essence, the stratospheric pathway involves a sequence of processes:

1. Aerosols from low-latitude volcanic eruptions absorb radiation and warm the tropical lower stratosphere.

2. Through thermal wind balance and eddy-mean flow interaction, this warming strengthens the winter stratospheric polar vortex (Hollowed et al., 2025; Paik et al., 2023).

3. The intensified vortex promotes a positive phase of the North Atlantic Oscillation (NAO), which subsequently generates warm surface temperature anomalies downstream over Eurasia (Hermanson et al., 2020).

This mechanism operates only if the eruption occurs on the equatorward side of the polar night jet, where the ascending branch of the stratospheric Brewer-Dobson circulation (Butchart, 2014) allows aerosols to persist longer in the stratosphere. The resulting surface impacts are limited to the extended boreal winter, when the stratospheric polar vortex is dynamically active.

Later observational and modeling studies noted several caveats to this mechanism. Observational studies of low-latitude eruptions in the last millennium found that warming was stronger during the second winter after eruptions rather than the first (Fischer et al., 2007) and that most eruptions were actually followed by cooling in subpolar Eurasia (Tejedor et al., 2024). The result reported by Fischer et al. (2007) is particularly difficult to explain, as aerosol concentrations are much lower in the second year after eruption than after the first. Furthermore, other sources of variability (either internal or forced) can overwhelm the volcano-induced NAO signal (Wunderlich and Mitchell, 2017; Tejedor et al., 2024).

Modeling studies of the response to low-latitude eruptions have produced conflicting results. These studies have examined large ensemble simulations from a single model (Bittner, 2015; Bittner et al., 2016; Thomas et al., 2009a, b; Toohey et al., 2014) or just a few models (e.g., three in Polvani et al., 2019), or historical simulations with all forcings included but with small model-ensemble sizes as part of the Coupled Model Intercomparison Project (CMIP; Driscoll et al., 2012; Zambri and Robock, 2016; Polvani and Camargo, 2020). Although the ensemble-mean response indicates some Eurasian warming in many of these studies (Zambri and Robock, 2016; Polvani et al., 2019), it is often weaker than the observed response. Furthermore, in some modeling studies the tropical stratospheric warming does not extend far enough poleward to affect the polar vortex (e.g. Bittner et al., 2016). However, when individual ensemble members are examined, many simulations show warming comparable to — or even greater than — the warming observed after the eruption. Other simulations show strong winter cooling despite identical aerosol forcing. One interpretation is that the observed warming is heavily influenced by internal climate variability and should not be interpreted as a direct response to volcanic aerosols (Polvani and Camargo, 2020; Weierbach et al., 2023). Very recently, Weber et al. (2026) analyzed historical simulations from 15 climate models with at least 10 ensemble members each, showing that most models capture the polar vortex response and simulate a significant, though model-dependent, Eurasian temperature response. This positive NAO response (Ortega et al., 2015; Sjolte et al., 2021) is likely associated with enhanced storminess over Europe (Andreasen et al., 2024), and specifically with enhanced storminess over Ireland evident in paleo-data during the Holocene (Orme et al., 2026).

Although there are studies that have demonstrated that even larger eruptions than those experienced in the past 150 years would show the signal more clearly (Azoulay et al., 2021; DallaSanta and Polvani, 2022), establishing statistical significance still requires many eruption events. For example, an eruption of 40 Tg(S) — a factor of 4 larger than Krakatoa and Pinatubo and larger than all but one known eruption of the last millennium — would require at least eight events to detect a statistically significant signal (DallaSanta and Polvani, 2022). Even for eruptions up to 80 Tg(S), the resulting forced winter warming remains smaller than one standard deviation of the natural year-to-year variability of Eurasian winter temperatures.

There is also a lack of consensus in the literature on whether low-latitude volcanic eruptions influence the phase of El Niño–Southern Oscillation (ENSO), among other modes of sea-surface temperature variability. Some paleo-reconstructions indicate that there is no relationship between volcanic eruptions and the phase of ENSO (Dee et al., 2020; Tejedor et al., 2024; Zhu et al., 2022), however others do find a relationship (McGregor et al., 2020b; D'Agostino et al., 2026). Models tend to simulate a transition to El Niño conditions within a few months after volcanic eruptions (Ohba et al., 2013; McGregor et al., 2020a; Ward et al., 2021; Dogar et al., 2023) and a La Niña event three years later (Maher et al., 2015), though this response can also be overwhelmed by internal variability (Weierbach et al., 2023). This near-immediate El Niño response becomes more apparent if the mean cooling of the tropics is subtracted (Ward et al., 2021). More recent modeling studies indicate that the effect of eruptions on ENSO is sensitive to ocean preconditioning, eruption magnitude and location, and the representation of air–sea feedbacks (Predybaylo et al., 2020; Ward et al., 2021; Weierbach et al., 2023). Finally, the ENSO response might act to intensify the downstream impacts on the Eurasian winter temperature response to volcanic eruptions. Specifically, Coupe and Robock (2021) argue that the existence of El Niño conditions in the tropical Pacific in 1991 was essential for triggering Eurasian winter warming after the eruption of Pinatubo. However, other studies found no evidence for El Niño influencing the Eurasian winter response following eruptions (Christiansen, 2008; Thomas et al., 2009b; Dogar et al., 2024; Weber et al., 2026).

This paper revisits these challenges and gaps using the model output of the Large Ensemble Single Forcing Model Intercomparison Project (LESFMIP) (Smith et al., 2022). The LESFMIP is composed of a coordinated series of historical model experiments in which large ensembles of global climate simulations are compiled under a single-forcing configuration. One single-forcing scenario is particularly relevant to these gaps, as it isolates the role of volcanic aerosols; all other forcing (greenhouse gases, other aerosols, solar radiation, and land use) are held fixed at preindustrial values. This separation of solar and volcanic forcings is crucial, as previous work indicates some aliasing. Specifically, Pinatubo erupted during high-solar radiation conditions, and this leads to ambiguities in attributing the tropical lower stratospheric warming and subsequent polar stratospheric response both in observations and in all-forcing simulations (Chiodo et al., 2014; Kuchar et al., 2017; Huo et al.,

https://doi.org/10.5194/egusphere-2026-3738
Preprint. Discussion started: 24 July 2026

2025). Krakatoa also erupted close to solar maximum, though the estimated amplitude of that solar maximum was relatively weak. This obstacle is overcome by the LESFMIP, which is designed around single-forcing experiments and therefore prevents aliasing of the solar and volcanic signals. Furthermore, LESFMIP is designed around large ensembles (at least 10 per model), which allows for distinguishing forced signals from the internal variability of the atmosphere. Of the modeling centers contributing output to the LESFMIP, eight performed >10 ensemble members with time-evolving volcanic aerosols only, and in total 200 ensemble members are available. These simulations cover the period 1850–2020 and so cover both the eruption of Pinatubo in 1991 and the eruption of Krakatoa in 1883.

The data used for this study and the methodology adopted are introduced in Section 2. Motivated by seemingly contradictory claims from different studies, we revisit the surface response to historical eruptions in Section 3. We then discuss implications for the observed response and for previous modeling studies in Section 4.

2 Methods

This paper focuses on model output contributed to the LESFMIP project, and specifically the eight models that have contributed *hist-volc* single forcing experiments following Phase 1 of the LESFMIP protocol. For each of these models, at least 10 ensemble members cover the period 1850 to 2020. The specific ensemble sizes for each model are shown in Table 1. Full details of the LESFMIP protocol can be found in Smith et al. (2022). The data is freely available on the Earth System Grid Federation (Cinquini et al., 2014, ESGF), and can be found as large ensembles of the DAMIP project (Gillett et al., 2016). In all, 200 ensemble members are available. In the main text, we analyze the responses to Pinatubo and Krakatoa together as compared to the mean climate in the five years prior to each eruption, and so we effectively have 400 independent samples of the atmospheric response to an explosive tropical volcanic eruption. The specification of the sulfur burden and effective radiation forcing in the CMIP6 aerosol input dataset is similar for both eruptions (Arfeuille et al., 2014; Aubry et al., 2026) and both are located in the tropics; nonetheless, we include in the supplemental material select figures with the response to each eruption separately. These figures indicate that Krakatoa had a stronger impact than Pinatubo.

Monthly raw output from the models was re-gridded to a common $2.5° \times 2.5°$ grid. The multi-model mean (MMM) response is evaluated by first computing the ensemble mean for each model and then averaging the eight ensemble means together. This gives each model an identical weight. Stippled areas on MMM figures indicate that at least 6 of 8 models agree with the MMM on the sign of the response. Stippling on the response for each model indicates that differences from the pre-eruption period are statistically significant at the 95% level based on a two-tailed Student-t test.

The 40 ensemble members of GISS-E2-1-G are composed of two separate model versions: p3f1 and p1f2. In physics version 1, aerosols and ozone are read in via pre-computed transient aerosol and ozone fields, and the aerosol indirect effect is parameterized. In physics version 3, atmospheric composition is calculated using a One-Moment Aerosol scheme which includes the aerosol impacts on clouds (Bauer et al., 2020). Forcing versions 1 and 2 differ in the handling of volcanic aerosol surface area density (Kelley et al., 2020). These differences do not appear to matter for our analysis, however: the U10hPa 60N zonally

https://doi.org/10.5194/egusphere-2026-3738
Preprint. Discussion started: 24 July 2026

averaged wind response in DJF in the two versions is mutually indistinguishable (4.27 m/s and 4.46 m/s). We therefore combine the two versions throughout this paper.

To analyse the storm track response after the Krakatoa and Pinatubo eruptions, we compute subseasonal variance using a 24-hour difference filter of daily sea level pressure (SLPDIFF) following the methodology proposed by Chang et al. (2012). This filter has a half-power point at periods of 1.2 and 6 days, and the results obtained based on this filter are very similar to those obtained using other commonly used band-pass filters (e.g. Chang et al., 2002). We compute monthly means of SLPDIFF and then aggregate to DJF seasonal means.

Observed near-surface temperature anomalies are sourced from Berkeley Earth (Rohde and Hausfather, 2020).

Table 1. Number of model ensemble members for the hist-volc experiments. ACC=ACCESS-ESM1-5, Can=CanESM5, CMCC=CMCC-CM2-SR5, GISS=GISS-E2-1-G, Had=HadGEM3-GC31-LL, MIROC=MIROC6, MPI=MPI-ESM1-2-LR, and Nor=NorESM2-LM

	ACC	Can	CMCC	GISS	Had	MIROC	MPI	Nor
hist-volc	10	30	10	40	50	10	30	20

3 Results

3.1 Multimodel mean response

We begin by considering the temperature response to Pinatubo and Krakatoa in Figure 1a-d. In the first winter after eruption, temperatures warm in the tropical lower stratosphere by up to 5.5 K. Warming extends into the subtropics, consistent with observations but with a stronger amplitude (Labitzke and McCormick, 1992; Hampson et al., 2006; Fujiwara et al., 2015). This signal is still evident, though weaker, in the following winter (∼1.5 years after the eruption; Figure 1b), and does not fully dissipate until more than 3 years have passed. The tropical troposphere cools in the first winter after eruption (Figure 1a). This cooling spreads to higher latitudes and strengthens in the following winter (1.5 years after eruption; Figure 1b) before weakening in the subsequent winters (Figure 1c, d).

The warming of the tropical lower stratosphere strengthens the meridional temperature gradient, which directly leads to an acceleration of zonal winds in the extratropical stratosphere and a stronger stratospheric polar vortex (Figure 1e-h). This response is evident in the first winter after eruption (Figure 1e) and to a lesser extent in the second (Figure 1f), before disappearing in later winters (Figure 1gh).

The surface temperature response to the two eruptions is shown in Figure 2a-d. Surface temperatures cool nearly everywhere in the first winter after eruption (Figure 2a), with high latitude Eurasia a notable exception. There, temperatures warm by up to 1 K, with a 0.74 K difference in temperature in the boxed region relative to the global average. In the second winter after eruption, temperatures in high latitude Eurasia are still warmer than the global average, though no longer anomalously warm relative to the pre-eruption period (Figure 2b). Eastern Canada and subtropical Eurasia are particularly cold relative to the global average, so the regional warming and cooling pattern still bears the hallmark of polar stratospheric vortex strengthening

https://doi.org/10.5194/egusphere-2026-3738
Preprint. Discussion started: 24 July 2026

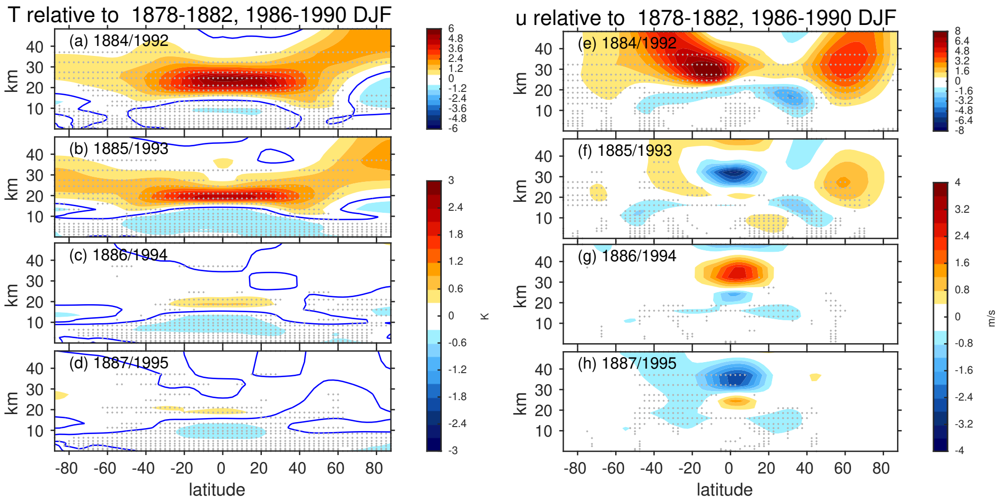

Figure 1. Multi-model mean latitude vs height zonally averaged (left) temperature and (right) zonal wind in response to the eruptions of Pinatubo and Krakatoa relative to the 5 years prior to each eruption in DJF. The top row considers the first winter after the eruption (DJF of 1991/1992 and 1883/1884), the second row the second winter after the eruption (DJF of 1992/1993 and 1884/1885), the third row the third winter after the eruption (DJF of 1993/1994 and 1885/1886), and the fourth row the fourth winter after the eruption (DJF of 1994/1995 and 1886/1887). The blue contour indicates the (a) -0.15K and (b-d) -0.075K isotherms. Note the different colorbar and contour interval for the top row as compared to the other rows. Stippling indicates where at least 6 of 8 models agree on the sign of the response (see Section 3.2 and Figure 6 for a discussion of each model). The responses for each eruption separately are in Supplemental Figure S1 and S2.

and a positive NAO (cf. figure 6 of Lawrence et al., 2020). Only in later winters, after the vortex response has gone away, is the cooling over high latitude Eurasia similar to or larger than the global cooling (Figure 2cd).

Previous work has suggested that the post-eruption response is stronger if the climate system is in an El Niño state before the eruption (Coupe and Robock, 2021). To evaluate this possibility, we group the available ensemble members by those with sea surface temperature (SST) anomalies in the Niño3.4 region greater than 0.5 K or less than -0.5 K in the May before the eruption and then consider the response in the following winters (Figure 2efgh for El Niño, Figure 2ijkl for La Niña). The Eurasian warming in the first winter after eruption is more pronounced for El Niño events (Figure 2e) than for all members, while the warming is weaker if we focus solely on La Niña (Figure 2i). These sensitivities are similar to those found by Coupe and Robock (2021).

Previous modeling work has noted a transition to El Niño in the winter following a volcanic eruption, though this effect appears somewhat less robust in paleoclimate proxies (see Introduction). If we focus on the raw surface temperature (or SSTs, not shown) in these models in the first winter after eruption (Figure 2a), the overall tropical cooling overwhelms any El Niño signal. Nonetheless, there is a small gap in the cooling in the west-central Pacific that hints at the possibility of an El Niño response. To more closely analyze this possibility, we turn to the ocean heat content integrated to 300 m depth in Figure 3. Figure 3a clearly shows an increase in ocean heat content in the tropical Central Pacific Ocean, consistent with typical El Niño

https://doi.org/10.5194/egusphere-2026-3738
Preprint. Discussion started: 24 July 2026

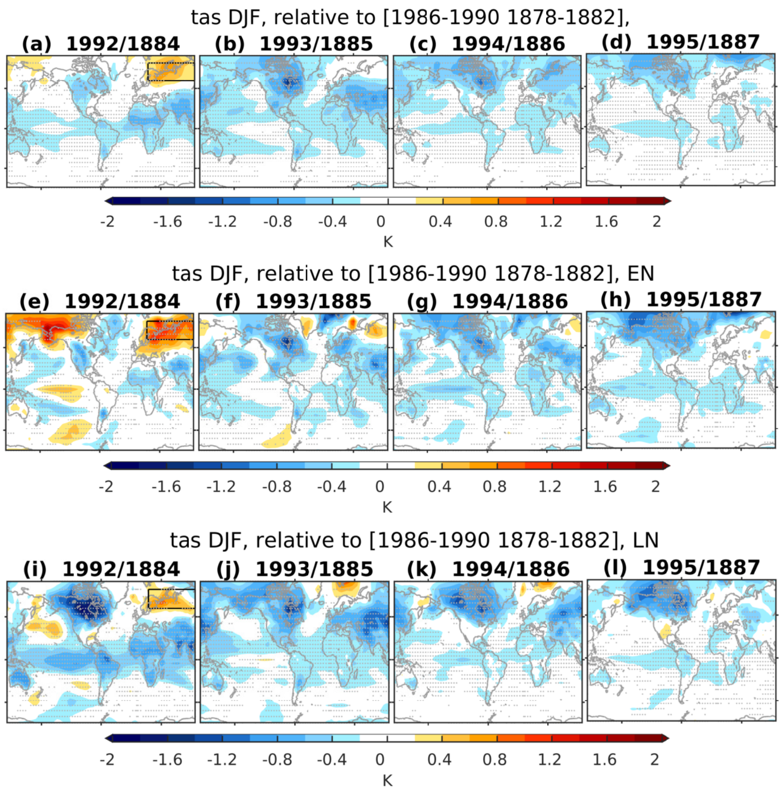

Figure 2. Surface temperature response in DJF to Pinatubo and Krakatoa relative to the five years preceding the eruption, for (a) the first winter after the eruption (1991/1992 and 1883/1884), (b) the second winter after the eruption (1992/1993 and 1884/1885), (c) the third winter after the eruption (1993/1994 and 1884/1885), (d) the fourth winter after the eruption (1994/1995 and 1885/1886). (e)-(h) as in (a)-(d) but for ensemble members with El Niño conditions in May before the eruption. (i)-(l) as in (a)-(d) but for ensemble members with La Niña conditions in May before the eruption. Stippling indicates where at least 6 of 8 models agree on the sign of the response (see Section 3.2 and Figure 8 for each model separately). The boxed region over Northern Eurasia is the focus region for Figures 9 and 10 (20-110°E, 60-75°N). Similar figures but for each eruption separately are in Supplemental Figure S3.

https://doi.org/10.5194/egusphere-2026-3738
Preprint. Discussion started: 24 July 2026

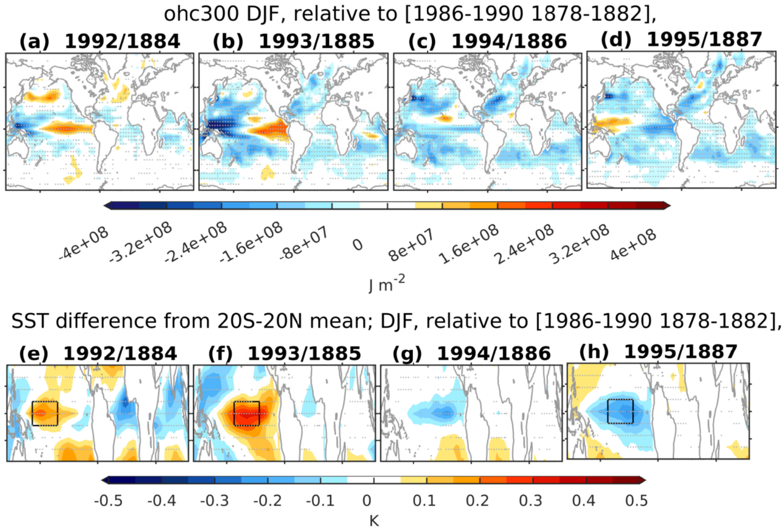

Figure 3. As in Figure 2a-d but for the (a-d) ocean heat content to 300m depth and for (e-h) sea surface temperatures relative to the 20S-20N mean. The box in (e) shows the Niño4 region, and in the box in (f) and (h) the Niño3.4 region. Similar figures but for each eruption separately are in Supplemental Figure S4.

features. If we focus on SSTs relative to the 20°S–20°N tropical mean (Figure 3e), the warming in the Niño4 region is robust across the models (cf. Figure 5 of Dogar et al., 2023). Hence, it appears that while the volcanic eruptions affect the ocean in such a way as to increase the likelihood of an El Niño, the surface cooling suppresses this response. Although the SST warming in the Niño4 region is statistically significant if we first remove the tropical-mean cooling signal, the surface warming in the Niño3.4 region is not (despite 400 degrees of freedom), even if we first remove the global mean or tropical-mean cooling (20°S–20°N). This difference indicates that volcanic eruptions tend to trigger a Central Pacific-type El Niño in the first year, and an Eastern Pacific-type El Niño in the second year (Figure 3f). Regardless of the initial ENSO state, a robust La Niña is present in the tropical Pacific three and four winters later (Figure 2cd,gh,kl). This effect, which is evident in both ocean heat content and SSTs (Figure 3cd,gh), is likely associated with the enhanced cooling signal over North America, which exceeds the global mean cooling (Figure 2cd).

Next, we characterize the dynamical response to the eruptions by examining sea level pressure (SLP; Figure 4). In the first winter, a clear positive NAO signal is evident in the Atlantic sector, with lower SLP at subpolar latitudes and higher SLP in the subtropics. SLP signals are also evident in the tropics: SLP is reduced in the tropical Pacific and increased over the Indian Ocean. Although this pattern resembles the canonical Southern Oscillation response typically evident during Central Pacific El Niño events (cf., figure 8 of Garfinkel et al., 2013), it is shifted to the west. In the North Pacific sector, SLP is anomalously high over Alaska and low over a broad span from Hawaii to California. This signal is again not a canonical El Niño response (to either Eastern Pacific- or Central Pacific-type events; Fig. 8 of Garfinkel et al., 2013), but is nonetheless likely associated with the El Niño-like lack of cooling in the Central Pacific (Fig. 2). To further diagnose this El Niño-like response in the first

https://doi.org/10.5194/egusphere-2026-3738
Preprint. Discussion started: 24 July 2026

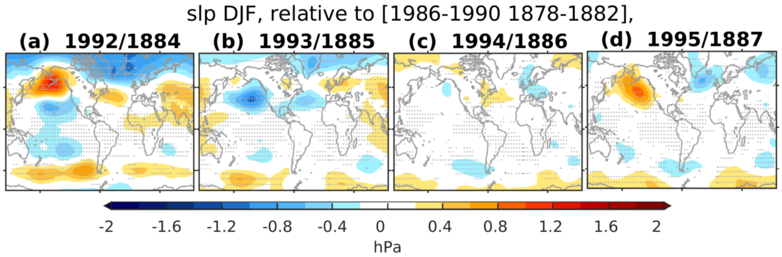

Figure 4. As in Figure 2 but for sea level pressure (SLP). Similar figures but for each eruption separately are in Supplemental Figure S5.

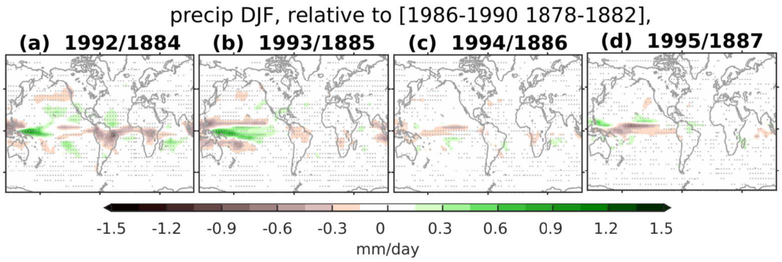

Figure 5. As in Figure 2 but for precipitation. Similar figures but for each eruption separately are in Supplemental Figure S6.

winter, we show the precipitation response in Figure 5. A precipitation dipole is evident in the tropical Pacific with decreased precipitation over most of the maritime continent, but the increased precipitation is limited to the West Pacific only. This pattern again differs from that expected for Eastern Pacific or Central Pacific El Niño events, in which precipitation impacts extend eastward into the Central Pacific as well (Figure 6 of Garfinkel et al., 2013). In addition to these tropical precipitation responses, the models simulate a drying over the Pacific Northwest and a wettening over the Southwestern United States and northern Mexico in the first year after eruption (Figure 5a). Although such signals somewhat resembles those typical of El Niño, the anomalies are shifted to the south of a canonical El Niño response.

In the second winter after the eruption, the NAO response is weaker but still present (Figure 4b). In the Pacific sector, the SLP response more closely resembles the canonical ENSO teleconnection: a low is evident over the Northeast Pacific, the gap in cooling in the tropical Pacific expands eastwards towards the Central–East Pacific (Figure 2b), the increase in ocean heat content is strongest in the East Pacific (Figure 3b), and the increased precipitation extends into the Central Pacific (Figure 5b). Finally, in the fourth year after eruption, the SLP, ocean heat content, surface temperature and precipitation patterns all resemble those typical of La Niña: ridging in the Northeast Pacific, pronounced surface cooling in the tropical East Pacific and Alaska, and reduced precipitation in the tropical Central Pacific (Figure 2d, 3d, 4d, 5d).

Thus far, we have focused on the multimodel mean response, which reveals a statistically significant response to eruptions in many parts of the world, including subpolar Eurasia. However, there are noteworthy differences among models and ensemble

https://doi.org/10.5194/egusphere-2026-3738
Preprint. Discussion started: 24 July 2026

members that have implications for interpreting both the observed response and the model responses presented in previous work. These differences are documented in the next section.

3.2 Contrasting the response across models and ensemble members

We begin by considering the magnitude of the zonally averaged temperature and wind response in the first winter in each model's ensemble mean ($\sim$6 months after eruption; Figure 6). In some models the tropical lower stratospheric warming approaches 8 K, while in others it peaks at $\sim$3 K. If we compare the response to Pinatubo only (Supplemental Figure S7), a similarly wide range is evident, with ACCESS and MIROC6 showing weaker responses than the other models. The models also disagree as to the polar stratospheric temperature response: HadGEM and CMCC (Figure 6ce) show a strong polar cooling. Consistent with the enhanced meridional temperature gradient, the zonal wind response near the polar vortex response is strongest in these two models. On the other hand, ACCESS and MIROC6 (Figure 6af) show no polar cooling at all and, consistent with this, the polar vortex response is weak. Model outputs from two of the modeling centers considered here — GISS and MPI — have been used in previous work on the stratospheric response to volcanic eruptions. These two models show responses that are close to the MMM with a weak cooling over the pole and a moderate strengthening of the polar vortex (Figure 6dg,lo).

To understand the source of the intermodel spread in the tropical stratospheric temperature response, we diagnose diabatic heating using the Q_1 framework (Yanai et al., 1973):

$$Q_1 = \frac{\partial T}{\partial t} + u\frac{\partial T}{\partial x} + v\frac{\partial T}{\partial y} + s\omega \quad (1)$$

where

$$s = -\frac{T}{\theta}\frac{\partial \theta}{\partial p}. \quad (2)$$

is the static stability and all other notation is standard (Sobel and Bretherton, 2000). The right-hand side of Equation 1 is computed from the monthly mean wind and temperature output, and allows for inferring the diabatic heating anomalies induced by the eruptions even though the diabatic heating directly computed by the models is unavailable.

The multimodel mean of Q_1 in the first winter after eruption as compared to the previous 5 winters is shown in Figure 7a. Volcanic eruptions lead to enhanced tropical diabatic heating, likely due to enhanced radiative absorption. In midlatitudes, on the other hand, there is diabatic cooling likely due to longwave (LW) cooling. While these responses are robust across models, the magnitude differs. We demonstrate this on the ordinate on Figure 7b, which shows the magnitude of the Q_1 heating in the tropical stratosphere in the boxed region on Figure 7a: the magnitude of the diabatic heating differs across models by a factor of four even though they use the same CMIP6 volcanic aerosol forcing. The abscissa of Figure 7b shows the magnitude of the tropical stratospheric temperature response, demonstrating a tight and statistically significant relationship between the Q_1 and temperature responses (r=0.94). The correlation is also strong (though not significant) between tropical Q_1 and the zonal wind response at 10hPa and 60°N (r=0.56). This suggests that models with a weaker diabatic heating response in the tropical stratosphere (e.g., ACCESS and MIROC) exhibit a weaker stratospheric response more generally.

https://doi.org/10.5194/egusphere-2026-3738
Preprint. Discussion started: 24 July 2026

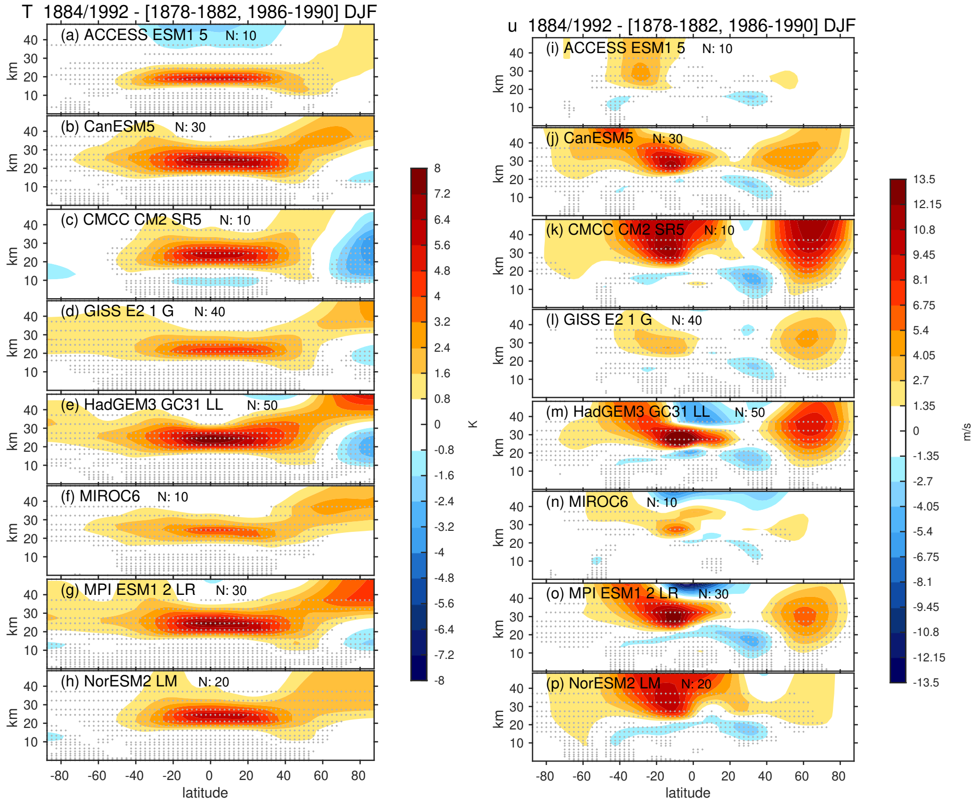

Figure 6. lat vs height of the U and T response to Pinatubo and Krakatoa, DJF, in the first winter after eruption, for each model. Stippling indicates regions where a null hypothesis of no effect can be rejected at the 95% confidence level using a two-tailed Student-t test. Supplemental Figure S7 shows the response to Pinatubo only.

This spread in the stratospheric response has implications for intermodel spread in the surface temperature response over subpolar Eurasia. We demonstrate this by showing the temperature response in each model in the first winter after eruption in Figure 8. The two models with the weakest polar vortex response (MIROC and ACCESS) also show cooling over subpolar Eurasia (Figure 8af), rather than the warming signal evident in the multimodel mean and reported by many previous modeling studies. Nonetheless, one MIROC6 member shows warming larger than was observed, and a second underestimates the warming by less than 10%. The two models with the strongest polar vortex acceleration — CMCC and HadGEM — show a pronounced warming over subpolar Eurasia, as do the other models. When the response is averaged over the boxed region in Figure 8, four of the models show a statistically significant warming (HadGEM, CMCC, MPI, and GISS-E2_1_G). The responses in GISS and MPI, the two models used in many previous studies on this topic (e.g., DallaSanta and Polvani, 2022; Azoulay et al., 2021; Qin et al., 2025), exceed the multimodel mean (Figure 8dg).

These responses are based on averaging over all available ensemble members, which acts to damp out internal variability. In reality, the observed anomalies following the two eruptions include both this forced signal plus internal variability. We now

https://doi.org/10.5194/egusphere-2026-3738
Preprint. Discussion started: 24 July 2026

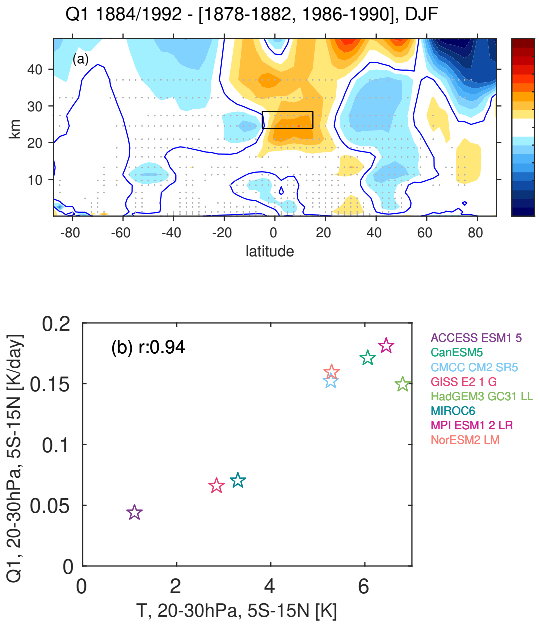

Figure 7. Multimodel mean Q_1 (see equation 1) response to Krakatoa and Pinatubo for (a) the first winter after the eruptions (1991/1992 and 1883/1884) relative to the 5 years before eruption. Stippling indicates where at least 6 of 8 models agree on the sign of the response. The -0.0125 K/day contour is indicated in blue. (b) the response of Q_1 in the tropical stratosphere (see boxed region in a) in each model contrasted with the temperature response in the same region. Correlations exceeding 0.84 are statistically significant at the 99% confidence level using a two-tailed student-t test.

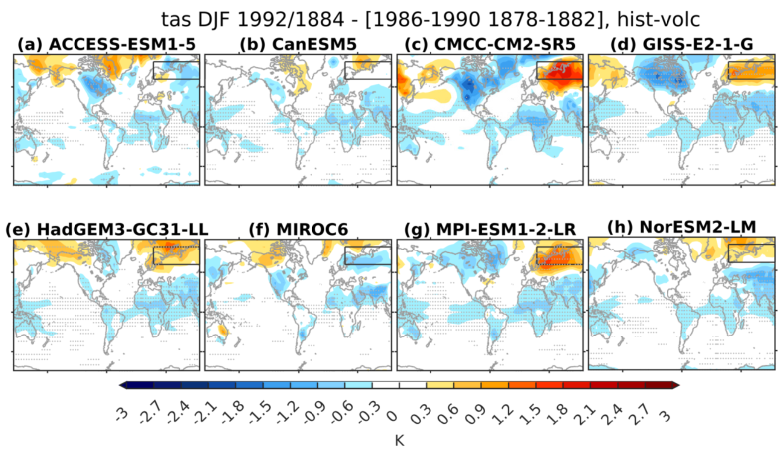

Figure 8. Surface temperature response in DJF to Pinatubo and Krakatoa relative to the five years preceding the eruption, for the first winter after the eruption (1991/1992 and 1883/1884) for each model separately. Stippling indicates regions where a null hypothesis of no effect can be rejected at the 95% confidence level using a two-tailed Student-t test. The box over Northern Eurasia marks the focus region for Figure 9 and 10 (20-110°E, 60-75°N).

https://doi.org/10.5194/egusphere-2026-3738
Preprint. Discussion started: 24 July 2026

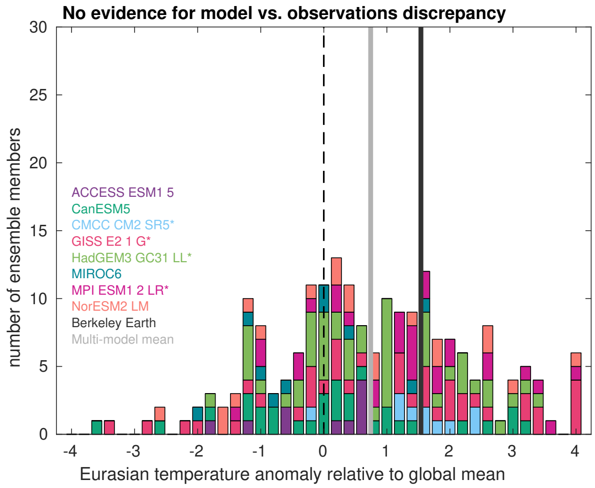

Figure 9. Surface temperature response to Pinatubo and Krakatoa in each of the 200 ensemble members in the boxed region over Northern Eurasia in Figure 2 (20-110°E, 60-75°N). The light gray line shows the multi-model mean, and the dark gray line the response based on the BEST observational analysis. Asterisks indicate models in which the warming relative to the global mean is statistically significant. In seven of eight models, at least one ensemble member has a response as large as that observed (ACCESS is the lone exception).

consider the salience of the forced signal in the modeling experiments. First, we consider the magnitude of the warming over high latitude Eurasia in each available ensemble member (Figure 9). There is a wide spread in the response, and while 134 of the 200 members show warming over high latitude Eurasia, the other 66 do not. While this is highly statistically significant (well above the 99.9%) based on a binomial test, it is clearly possible for internal variability to mask the forced response from volcanoes. The observed temperature anomaly from BEST is 1.54 K (dark gray line). Although this value exceeds the mean averaged over all members by about a factor two (thin gray line: 0.74 K), there is no evidence for a model vs. observations discrepancy. Furthermore, there is substantial observational uncertainty as to the magnitude of the Krakatoa-induced warming (Tejedor et al., 2024).

We have 200 ensemble members and thus 400 independent realizations of the climate system response to volcanic eruptions of the magnitude of Pinatubo or Krakatoa, a factor of 20 larger than that analyzed by DallaSanta and Polvani (2022), a factor of four larger than that analyzed by Azoulay et al. (2021), and a factor of two larger than that analyzed by Qin et al. (2025). Using the entirety of this data, we can conclude with confidence that subpolar Eurasia exhibits a tendency to warm following an eruption. This finding, however, raises an important question: how large must an ensemble be for this response to emerge robustly above internal variability? We address this question using a bootstrapping approach, in which we subsample from the large ensemble (Figure 10). Specifically, we select with replacement 2 events with resampling from the available 400, and compute the difference in Eurasian surface temperature between the first winter after the eruption and the previous five winters. We repeat this 1000 times, thereby generating an uncertainty estimate for the mean response. Next, we subselect 4 events and repeat 5000 times, then 6, and so on until we randomly subselect 400 events with resampling. On each panel we indicate how

https://doi.org/10.5194/egusphere-2026-3738
Preprint. Discussion started: 24 July 2026

many months must be selected for the 2.5% lower bound of the uncertainty to not include 0 K. At minimum, 62 eruptions are needed to confidently identify a robust warming of Eurasian surface temperature (Figure 10a). This result is very similar to the number of 10 Tg(S) eruptions required in the GISS simulations of DallaSanta and Polvani (2022) before significance is achieved (estimated to be 64 events). If we instead ask the question: how many eruptions are needed before the warming of Eurasian surface temperature robustly emerges from the global mean cooling, we find that 34 eruptions are needed (Figure 10b). However, this amount of data would still only weakly constrain the amplitude of the surface temperature response, even though the mean of the bootstrapped estimates (blue line) is insensitive to the number of eruptions included in the average. Even if we exclude MIROC6 and ACCESS (the two models without a stratospheric polar vortex response) in the subsampling, we still require 48 eruptions to confidently identify a significant warming of Eurasian surface temperature relative to the 5-year pre-eruption baseline and 28 eruptions to confidently identify a significant warming relative to the global mean cooling.

Finally, we adopt a similar procedure to quantify how many eruptions are needed before the Central Pacific El Niño signal in the first winter after eruption becomes robust (Figure 10c). We find that 106 eruptions are needed, suggesting that this effect could be easily missed by paleoclimate reconstructions with just $\sim$ 20 such events or by paleo-proxies that focus on the Niño3.4 region, where we do not find any warming. Furthermore, the Niño4 warming is only robust if we first remove the tropical mean cooling. The Eastern Pacific El Niño signal in the second winter requires 72 eruptions to emerge and so is a more robust feature than the year-1 response (Figure 10d), while the La Niña signal in the fourth winter after eruption becomes robust with only 48 eruptions (Figure 10e). Hence, the most robust ENSO response is the La Niña signal in the fourth winter. Previous modeling studies with smaller samples or paleoclimate studies with $\sim$ 20 events likely could have missed this response.

3.3 Storm Track response

Next, we consider the storm track response to the eruptions of Krakatoa and Pinatubo. Figure 11 shows zonal-mean SLPDIFF as a proxy for storm track changes for winters after the Krakatoa (upper row; a–d) and Pinatubo (lower row; e–h) eruptions. The MMM reveals a statistically significant weakening of storm activity in midlatitudes (30–50°N and 40–60°S) in the first winter after Krakatoa (Fig. 11a) and Pinatubo (Fig. 11e). While models simulate an increase in storm track activity at higher NH latitudes during the first winter after Krakatoa, the response is not statistically significant, primarily because ACCESS simulates the opposite response relative to the other models. The ACCESS model also features the weakest tropical stratospheric temperature response (see Fig. 6a) and little vortex strengthening (see Fig. 6i). The models show no agreement on storm track strengthening at higher latitudes in the first winter after Pinatubo.

The poleward shift in storm-track activity corresponds to the positive NAO response (see above). Andreasen et al. (2024) linked it to steepening of the isentropic slope due to a larger meridional temperature gradient, as well as a lower tropopause driven by a combination of tropical stratospheric warming and surface cooling. Regionally, this shift occurs mainly in the Pacific and Atlantic during the first winter after Krakatoa and Pinatubo (see Fig. S10a,e), respectively. Simulated storm track activity weakens after Pinatubo across the Pacific.

The second winter is characterised by the same signature from the zonal mean perspective (see Fig. 11b,f) and even regionally (see Fig. S10b,f). However, models do not simulate any statistically significant response in the zonal mean. Interestingly, even

https://doi.org/10.5194/egusphere-2026-3738
Preprint. Discussion started: 24 July 2026

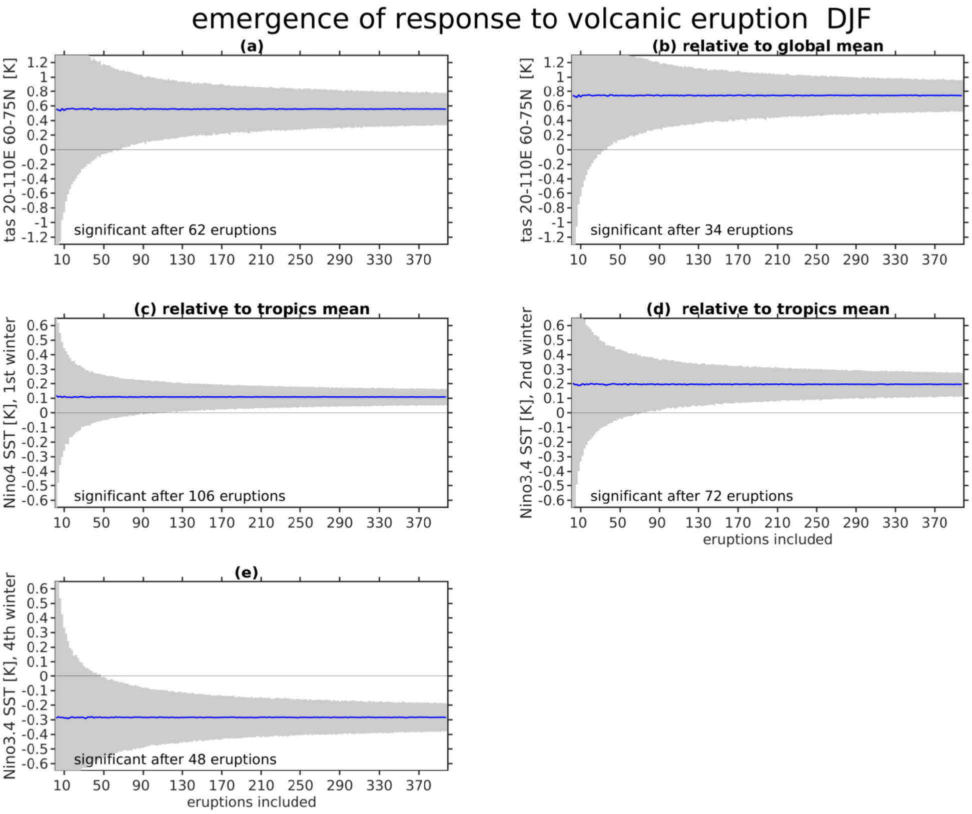

Figure 10. Emergence of the surface temperature response to Pinatubo and Krakatoa as compared to the five winters before eruption upon subsampling the full ensemble to quantify the added value of a large ensemble for quantifying teleconnection strength. (a,b) subpolar Eurasia warming (see boxed region in Figure 2) in the first winter after eruption (a) without and (b) with subtraction of the global mean cooling; (c) Niño4 region in the first winter after eruption relative to the tropical-mean cooling; (d) Niño3.4 region in the second winter after eruption relative to the tropical-mean cooling; and (e) Niño3.4 region in the fourth winter after eruption. Blue lines indicate the mean of the 1000 bootstrapped samples.

https://doi.org/10.5194/egusphere-2026-3738
Preprint. Discussion started: 24 July 2026

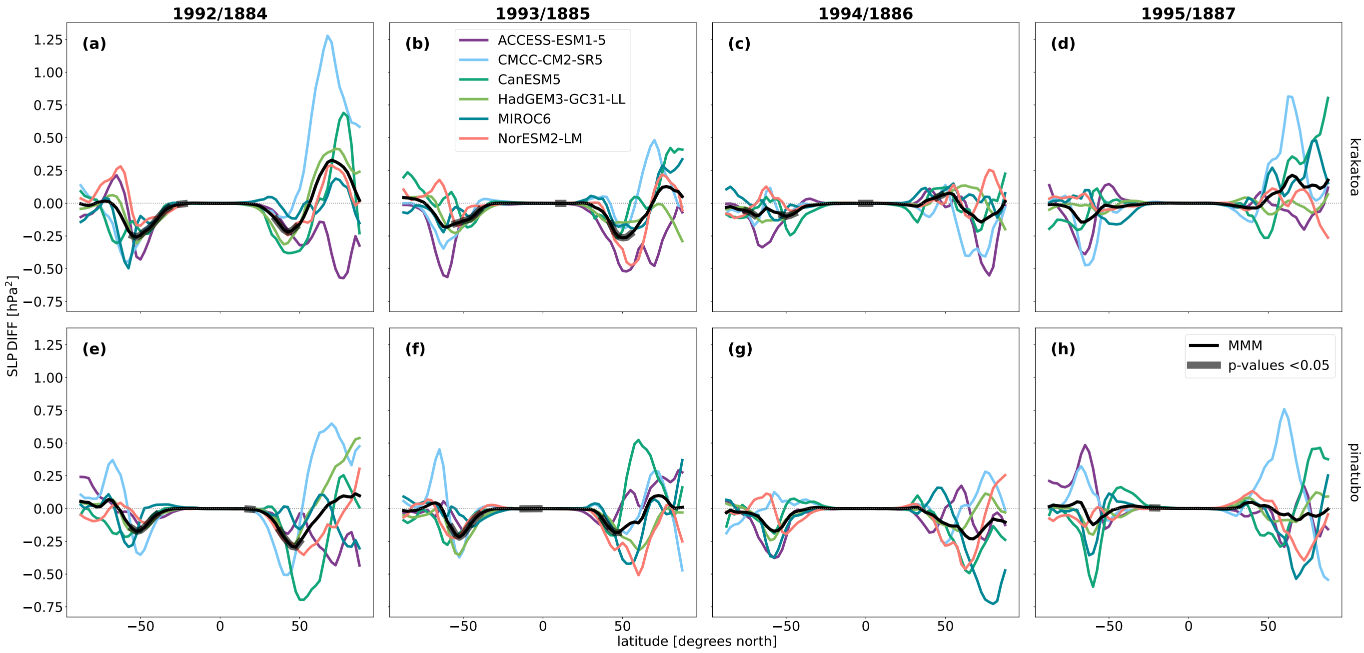

Figure 11. 24-hour difference filtered boreal-winter variance of sea level pressure (SLP) and its response to Krakatoa (upper row) and Pinatubo (lower row) for (a,e) the first winters after the eruptions (1991/1992 and 1883/1884), (b,f) the second winters after the eruptions (1992/1993 and 1884/1885), (c,g) the third winters after the eruptions (1993/1994 and 1884/1885), and (d,h) the fourth winters after the eruptions (1994/1995 and 1885/1886). Coloured and black thin lines represent individual and multi-model mean (MMM) responses, respectively. Thicker black lines show where the p-values of the t-test < 0.05.

in the fourth winter after Krakatoa, we find stronger storm activity in Northern Europe and weaker activity in the Mediterranean area (see Fig. S10d), respectively. Since we do not detect any multi-model response in zonal wind in DJF of 1887 (see Fig. 1h), we may argue that the diabatically forced changes do not play any role; this enhanced storm activity may be instead be driven by a shortwave pathway manifesting several winters after the eruption (Andreasen et al., 2026; Weber et al., 2026; Guðlaugsdóttir et al., 2025).

4 Discussion and Conclusions

Volcano eruptions have global impacts on climate from monthly to centennial timescales, and understanding these impacts can help with prediction and planning in the case of a volcanic eruption today (Hermanson et al., 2020; D'Agostino et al., 2026). We focus here on large ensembles from eight modeling centers made available as part of the LESFMIP project in which the only time varying forcing is volcanic aerosols, to isolate the climate response without any aliasing from, e.g., solar variability. In total, we have 200 realizations of the response to the eruptions of Pinatubo (1991) and Krakatoa (1883), the two strongest tropical eruptions since 1850, which we aggregate to form a sample size of 400 eruptions.

https://doi.org/10.5194/egusphere-2026-3738
Preprint. Discussion started: 24 July 2026

Many of the responses are consistent with previous work: the Arctic polar vortex strengthens, storm tracks shift polewards, subpolar Eurasia warms, and El Niño follows shortly after an eruption. However, all of these responses require at least 30 modeled eruptions before we can confidently conclude with 95% certainty that differences from the pre-eruption period do not reflect sampling variability. However, there are also a number of conclusions that appear not to have been noted before:

- The El Niño response to eruptions in year one after eruption is not a canonical East Pacific response. The sea surface warming is evident in the Niño4 region only, while the Niño3.4 region experiences no warming even if we remove the tropical-mean cooling. Such an effect also appears in Figure 5 of Dogar et al. (2023). This concentration of SST warming in the West–Central Pacific leads to a precipitation response that is also shifted westward of the canonical ENSO response. The resulting North Pacific teleconnection is therefore in quadrature with expected El Niño teleconnections: it resembles the North Pacific Oscillation, the second empirical orthogonal function (EOF) in the Pacific sector, rather than the first EOF with a deepened Aleutian low (Chen et al., 2024). The precipitation impacts over Western North America are shifted to the south of what typically occurs during El Niño. These effects are likely due to the fact that volcanoes lead to an overall surface cooling, and the convective response to SST anomalies may have some threshold dependence (Hu et al., 2023). It could also result from the stratospheric polar vortex response, which has been shown to influence the Pacific sector in many climate models (Dai et al., 2023, 2024). Either way, this result has implications for attempts to use paleoclimate proxies to reconstruct whether historical eruptions led to ENSO, if these reconstructions assume that the response will be similar to naturally occurring events. Furthermore, it suggests that previous studies that have focused exclusively on the Niño3.4 index (He et al., 2026) will underestimate the ENSO response.

- The LESFMIP models show a wide spread in the magnitude of the volcanic response in both the stratosphere and troposphere, including in tropical lower stratospheric temperatures where one might expect the responses to be more similar. Understanding the sources of this spread is crucial, but is difficult to achieve given the general unavailability of related output from the LESFMIP models. The best we can do is to infer the diabatic heating using the Q_1 framework, which reveals that models with weak tropical stratospheric warming also feature weak diabatic heating anomalies (Figure 7). This subsequently leads to diversity across models in the stratospheric polar response. In particular, two models show essentially no ensemble-mean polar vortex response, although individual ensemble members do simulate a stronger vortex and Eurasian warming. We do not have the requisite data (e.g. Hollowed et al., 2025) to diagnose how the westerly anomaly reaches towards the pole, or equivalently what sets the latitude at which the meridional temperature gradient peaks. Nonetheless, some insight on these differences can be gained by contrasting the DJF response in Figure 6 with the JJA response in Supplemental Figure S9. The two models with the weakest tropical stratospheric temperature response in DJF (MIROC and ACCESS) also have the weakest response in JJA, however the differences among models are less pronounced in JJA. There is more agreement across models as to the polar vortex response: in particular, all eight models show a strengthened austral polar vortex. Westerlies are also enhanced in the subtropical NH stratosphere. These JJA results support the core hypothesis that tropical volcanic eruptions enhance meridional temperature gradients in the

https://doi.org/10.5194/egusphere-2026-3738
Preprint. Discussion started: 24 July 2026

stratosphere and accelerate zonal winds, and suggest that the large model spread in DJF may be due to compensating effects from eddies in some models.

- For the figures in the main text, we aggregate the responses to Pinatubo and Krakatoa in order to increase the sample size. However, the CMIP6 aerosol forcing for Krakatoa was slightly larger than that for Pinatubo (Aubry et al., 2026); consistent with this, the resulting response is stronger for most of the key metrics discussed in the paper, including the tropical lower stratospheric and polar vortex responses (Supplemental Figure S1, S2, S7, S8), the subpolar Eurasian warming response (Supplemental Figure S3), and the ENSO response (Supplemental Figure S4). The net effect is that the SLP patterns forced by the two eruptions exhibit differences in much of the midlatitudes (Supplemental Figure S5), likely due to differences in the polar vortex response and in the tropical precipitation response (Supplemental Figure S6).

Some studies have indicated that models can systematically underestimate the real response to external forcings, especially in the atmospheric circulation of the North Atlantic (Eade et al., 2014; Scaife and Smith, 2018). Specifically, Hermanson et al. (2020) showed that the SLP response to volcanic forcing in the first DJF in the Atlantic region of CMIP5 decadal predictions was about seven times weaker than observations. Certainly, biases in model simulations of the North Atlantic climate may also affect our investigation of the causal relationship between strong volcanic eruptions and winter warming. Therefore, improving the performance of models in simulating the mid-to-high-latitude mean state and variability will be crucial for advancing research on the climate effects of volcanic eruptions, especially their impacts on mid-to-high-latitude climates. Better representations of volcanic eruption forcing in future models will also be essential. Ongoing work is aimed at assessing the ability of these models to faithfully represent stratosphere–troposphere coupling in these and other LESFMIP experiments.

https://doi.org/10.5194/egusphere-2026-3738
Preprint. Discussion started: 24 July 2026

Data availability. All simulation data used in this study is available on the Earth System Grid Federation (ESGF; https://aims2.llnl.gov/search; Cinquini et al., 2014). The fifth generation ECMWF atmospheric reanalysis (ERA5) can be downloaded from the Climate Data Source from Copernicus (https://cds.climate.copernicus.eu/datasets) and is referenced in the text as Hersbach et al. (2020). This work used JASMIN, the UK's collaborative data analysis environment (https://www. jasmin.ac.uk; Lawrence et al., 2013).

Author contributions. CIG performed the analysis for most figures and wrote the paper. AK contributed Figure 11 and wrote the accompanying text. JSW performed the Q1 analysis. DA managed and downloaded the data, and created earlier versions of figures 2, 4, 5, and 7. SO assisted in the overall framing of the paper and the LESFMIP project. All authors helped with editing the manuscript

Competing interests. The authors declare no competing interests.

Acknowledgements. C.I.G is supported by the ISF-NSFC joint research program (ISF grant No. 3065/23. SO would like to acknowledge support from the UK NERC NE/Y000048/1 and CANARI projects. Correspondence should be addressed to C.I.G. (email: chaim.garfinkel@mail.huji.ac.il).

https://doi.org/10.5194/egusphere-2026-3738
Preprint. Discussion started: 24 July 2026

References

Andreasen, L. S., Cornér, J., Abbott, P. M., Sinclair, V. A., Riede, F., and Timmreck, C.: Changes in Northern Hemisphere extra-tropical cyclone frequency following volcanic eruptions, 3, 025 002, https://doi.org/10.1088/2752-5295/ad2c0e, 2024.

Andreasen, L. S., Shaw, T. A., Günther, M., and Timmreck, C.: Independent Short- and Longwave Pathways for a Zonally Asymmetric Northern Hemisphere Temperature Response to Tropical Volcanic Eruptions, Geophysical Research Letters, 53, e2025GL117 680, https://doi.org/10.1029/2025GL117680, 2026.

Arfeuille, F., Weisenstein, D., Mack, H., Rozanov, E., Peter, T., and Brönnimann, S.: Volcanic forcing for climate modeling: a new microphysics-based data set covering years 1600–present, Climate of the Past, 10, 359–375, https://doi.org/10.5194/cp-10-359-2014, 2014.

Aubry, T. J., Toohey, M., Khanal, S., Chim, M. M., Verkerk, M., Johnson, B., Schmidt, A., Kovilakam, M., Sigl, M., Nicholls, Z., Thomason, L., Naik, V., Rieger, L., Stiller, D., Ziegler, E., Durack, P., and Smith, I. H.: Stratospheric aerosol forcing for CMIP7 – Part 1: optical properties for pre-industrial, historical, and scenario simulations, Geoscientific Model Development, 19, 3725–3756, https://doi.org/10.5194/gmd-19-3725-2026, 2026.

Azoulay, A., Schmidt, H., and Timmreck, C.: The Arctic polar vortex response to volcanic forcing of different strengths, J. Geophys. Res. Atmos., 126, e2020JD034 450, https://doi.org/10.1029/2020JD034450, 2021.

Bauer, S. E., Tsigaridis, K., Faluvegi, G., Kelley, M., Lo, K. K., Miller, R. L., Nazarenko, L., Schmidt, G. A., and Wu, J.: Historical (1850-2014) aerosol evolution and role on climate forcing using the GISS ModelE2.1 contribution to CMIP6, Journal of Advances in Modeling Earth Systems, 12, e2019MS001 978, https://doi.org/10.1029/2019MS001978, 2020.

Bittner, M.: On the discrepancy between observed and simulated dynamical responses of Northern Hemisphere winter climate to large tropical volcanic eruptions, Ph.D. thesis, University of Hamburg, https://pure.mpg.de/rest/items/item_2239264/component/file_2239290/content, 2015.

Bittner, M., Schmidt, H., Timmreck, C., and Sienz, F.: Using a large ensemble of simulations to assess the Northern Hemisphere stratospheric dynamical response to tropical volcanic eruptions and its uncertainty, Geophys. Res. Lett., 43, 9324–9332, https://doi.org/10.1002/2016GL070587, 2016.

Butchart, N.: The Brewer-Dobson circulation, Reviews of Geophysics, 52, 157–184, https://doi.org/https://doi.org/10.1002/2013RG000448, 2014.

Chang, E. K. M., Lee, S., and Swanson, K. L.: Storm Track Dynamics, 15, 2163–2183, https://doi.org/10.1175/1520-0442(2002)015<02163:STD>2.0.CO;2, 2002.

Chang, E. K. M., Guo, Y., and Xia, X.: CMIP5 multimodel ensemble projection of storm track change under global warming, Journal of Geophysical Research: Atmospheres, 117, https://doi.org/https://doi.org/10.1029/2012JD018578, 2012.

Chen, S., Chen, W., Wu, R., Yu, B., and Ying, J.: Joint impacts of winter North Pacific Oscillation and early spring Aleutian Low intensity on the following winter ENSO, Climate Dynamics, 62, 257–276, 2024.

Chiodo, G., Marsh, D. R., Garcia-Herrera, R., Calvo, N., and García, J. A.: On the detection of the solar signal in the tropical stratosphere, Atmospheric Chemistry and Physics, 14, 5251–5269, https://doi.org/10.5194/acp-14-5251-2014, 2014.

Christiansen, B.: Volcanic eruptions, large-scale modes in the Northern Hemisphere, and the El Niño–Southern Oscillation, J. Climate, 21, 910–922, https://doi.org/10.1175/2007JCLI1657.1, 2008.

https://doi.org/10.5194/egusphere-2026-3738
Preprint. Discussion started: 24 July 2026

Cinquini, L., Crichton, D., Mattmann, C., Harney, J., Shipman, G., Wang, F., Ananthakrishnan, R., Miller, N., Denvil, S., Morgan, M., et al.: The Earth System Grid Federation: An open infrastructure for access to distributed geospatial data, Future Generation Computer Systems, 36, 400–417, 2014.

Coupe, J. and Robock, A.: The influence of stratospheric soot and sulfate aerosols on the Northern Hemisphere wintertime atmospheric circulation, J. Geophys. Res., 126, e2020JD034 513, https://doi.org/10.1029/2020JD034513, 2021.

Dai, Y., Hitchcock, P., and Simpson, I. R.: Dynamics and impacts of the North Pacific eddy-driven jet response to sudden stratospheric warmings, Journal of Climate, 36, 865–884, 2023.

Dai, Y., Hitchcock, P., and Simpson, I. R.: What Drives the Spread and Bias in the Surface Impact of Sudden Stratospheric Warmings in CMIP6 Models?, Journal of Climate, 37, 3917 – 3942, https://doi.org/10.1175/JCLI-D-23-0622.1, 2024.

DallaSanta, K. and Polvani, L. M.: Volcanic stratospheric injections up to 160 Tg(S) yield a Eurasian winter warming indistinguishable from internal variability, Atmos. Chem. Phys., 22, 8843–8862, https://doi.org/10.5194/acp-22-8843-2022, 2022.

Dee, S. G., Cobb, K. M., Emile-Geay, J., Ault, T. R., Edwards, R. L., Cheng, H., and Charles, C. D.: No consistent ENSO response to volcanic forcing over the last millennium, Science, 367, 1477–1481, https://doi.org/10.1126/science.aax2000, 2020.

Dogar, M. M., Hermanson, L., Scaife, A. A., Visioni, D., Zhao, M., Hoteit, I., Graf, H.-F., Dogar, M. A., Almazroui, M., and Fujiwara, M.: A review of El Niño Southern Oscillation linkage to strong volcanic eruptions and post-volcanic winter warming, Earth Systems and Environment, 7, 15–42, 2023.

Dogar, M. M., Fujiwara, M., Zhao, M., Ohba, M., and Kosaka, Y.: ENSO and NAO Linkage to Strong Volcanism and Associated Post-Volcanic High-Latitude Winter Warming, Geophysical Research Letters, 51, e2023GL106 114, https://doi.org/https://doi.org/10.1029/2023GL106114, e2023GL106114 2023GL106114, 2024.

Driscoll, S., Bozzo, A., Gray, L. J., Robock, A., and Stenchikov, G.: Coupled Model Intercomparison Project 5 (CMIP5) simulations of climate following volcanic eruptions, J. Geophys. Res., 117, D17 105, https://doi.org/10.1029/2012JD017607, 2012.

D'Agostino, R., Fang, S.-W., Khodri, M., Pausata, F. S., Tejedor, E., Timmreck, C., and Zanchettin, D.: The Impact of Volcanic Eruptions on Tropical Hydroclimate, Annual Review of Earth and Planetary Sciences, https://doi.org/https://doi.org/10.1146/annurev-earth-071025-112048, 2026.

Eade, R., Smith, D., Scaife, A., Wallace, E., Dunstone, N., Hermanson, L., and Robinson, N.: Do seasonal-to-decadal climate predictions underestimate the predictability of the real world?, Geophysical research letters, 41, 5620–5628, 2014.

Fischer, E. M., Luterbacher, J., Zorita, E., Tett, S. F. B., Casty, C., and Wanner, H.: European climate response to tropical volcanic eruptions over the last half millennium, Geophys. Res. Lett., 34, L05 707, https://doi.org/10.1029/2006GL027992, 2007.

Fujiwara, M., Hibino, T., Mehta, S. K., Gray, L., Mitchell, D., and Anstey, J.: Global temperature response to the major volcanic eruptions in multiple reanalysis data sets, Atmospheric Chemistry and Physics, 15, 13 507–13 518, https://doi.org/10.5194/acp-15-13507-2015, 2015.

Garfinkel, C., Hurwitz, M., Waugh, D., and Butler, A.: Are the teleconnections of Central Pacific and Eastern Pacific El Niño distinct in boreal wintertime?, Climate dynamics, 41, 1835–1852, 2013.

Gillett, N. P., Shiogama, H., Funke, B., Hegerl, G., Knutti, R., Matthes, K., Santer, B. D., Stone, D., and Tebaldi, C.: The detection and attribution model intercomparison project (DAMIP v1. 0) contribution to CMIP6, Geoscientific Model Development, 9, 3685–3697, 2016.

Graft, H.-F., Kirchner, I., Robock, A., and Schult, I.: Pinatubo eruption winter climate effects: Model versus observations, Climate Dyn., 9, 81–93, https://doi.org/10.1007/BF00210011, 1993.

https://doi.org/10.5194/egusphere-2026-3738
Preprint. Discussion started: 24 July 2026

Guðlaugsdóttir, H., Peings, Y., Zanchettin, D., and Magnusdottir, G.: Stratospheric Circulation Response to Large Northern Hemisphere High-Latitude Volcanic Eruptions in a Global Climate Model, Atmospheric Chemistry and Physics, 25, 3961–3980, https://doi.org/10.5194/acp-25-3961-2025, 2025.

Hampson, J., Claud, C., Keckhut, P., and Hauchecorne, A.: The dynamical influence of the Pinatubo eruption in the subtropical stratosphere, Journal of Atmospheric and Solar-Terrestrial Physics, 68, 1600–1608, https://doi.org/https://doi.org/10.1016/j.jastp.2006.05.009, 2006.

He, Z., Tejedor, E., Smerdon, J. E., Vuille, M., Polvani, L. M., Seager, R., and Sugiura, I.: Comparison of Global Climatic Responses to Large Tropical Volcanic Eruptions over the Last Millennium in Paleoclimatic Reconstructions and Model Simulations, Journal of Climate, 39, 1295 – 1313, https://doi.org/10.1175/JCLI-D-25-0179.1, 2026.

Hermanson, L., Bilbao, R., Dunstone, N., Ménégoz, M., Ortega, P., Pohlmann, H., Robson, J. I., Smith, D. M., Strand, G., Timmreck, C., Yeager, S., and Danabasoglu, G.: Robust Multiyear Climate Impacts of Volcanic Eruptions in Decadal Prediction Systems, Journal of Geophysical Research: Atmospheres, 125, e2019JD031 739, https://doi.org/https://doi.org/10.1029/2019JD031739, e2019JD031739 10.1029/2019JD031739, 2020.

Hollowed, J. P., Jablonowski, C., Ehrmann, T., Bull, D., Wagman, B., and Hillman, B.: Volcanic aerosol modification of the stratospheric circulation in E3SMv2 – Part 1: Wave–mean flow interaction, Atmospheric Chemistry and Physics, 25, 11 025–11 049, https://doi.org/10.5194/acp-25-11025-2025, 2025.

Hu, S., Xie, S.-P., Seager, R., and Cane, M. A.: Spatial and seasonal variations of sea surface temperature threshold for tropical convection, Journal of Climate, 36, 4899–4912, 2023.

Huo, W., Spiegl, T., Wahl, S., Matthes, K., Langematz, U., Pohlmann, H., and Kröger, J.: Assessment of the 11-year solar cycle signals in the middle atmosphere during boreal winter with multiple-model ensemble simulations, Atmospheric Chemistry and Physics, 25, 2589–2612, 2025.

Kelley, M., Schmidt, G. A., Nazarenko, L. S., Bauer, S. E., Ruedy, R., Russell, G. L., Ackerman, A. S., Aleinov, I., Bauer, M., Bleck, R., Canuto, V., Cesana, G., Cheng, Y., Clune, T. L., Cook, B. I., Cruz, C. A., Del Genio, A. D., Elsaesser, G. S., Faluvegi, G., Kiang, N. Y., Kim, D., Lacis, A. A., Leboissetier, A., LeGrande, A. N., Lo, K. K., Marshall, J., Matthews, E. E., McDermid, S., Mezuman, K., Miller, R. L., Murray, L. T., Oinas, V., Orbe, C., García-Pando, C. P., Perlwitz, J. P., Puma, M. J., Rind, D., Romanou, A., Shindell, D. T., Sun, S., Tausnev, N., Tsigaridis, K., Tselioudis, G., Weng, E., Wu, J., and Yao, M.-S.: GISS-E2.1: Configurations and Climatology, Journal of Advances in Modeling Earth Systems, 12, e2019MS002 025, https://doi.org/https://doi.org/10.1029/2019MS002025, e2019MS002025 10.1029/2019MS002025, 2020.

Kirchner, I., Stenchikov, G. L., Graf, H.-F., Robock, A., and Antuña, J. C.: Climate model simulation of winter warming and summer cooling following the 1991 Mount Pinatubo volcanic eruption, J. Geophys. Res., 104, 19 039–19 055, https://doi.org/10.1029/1999JD900213, 1999.

Kodera, K.: Influence of volcanic eruptions on the troposphere through stratospheric dynamical processes in the Northern Hemisphere winter, J. Geophys. Res., 99, 1273–1282, https://doi.org/10.1029/93JD02731, 1994.

Kuchar, A., Ball, W. T., Rozanov, E. V., Stenke, A., Revell, L., Miksovsky, J., Pisoft, P., and Peter, T.: On the aliasing of the solar cycle in the lower stratospheric tropical temperature, Journal of Geophysical Research: Atmospheres, 122, 9076–9093, https://doi.org/https://doi.org/10.1002/2017JD026948, 2017.

Labitzke, K. and McCormick, M. P.: Stratospheric temperature increases due to Pinatubo aerosols, Geophysical Research Letters, 19, 207–210, https://doi.org/https://doi.org/10.1029/91GL02940, 1992.

https://doi.org/10.5194/egusphere-2026-3738
Preprint. Discussion started: 24 July 2026

Lawrence, Z. D., Perlwitz, J., Butler, A. H., Manney, G. L., Newman, P. A., Lee, S. H., and Nash, E. R.: The Remarkably Strong Arctic Stratospheric Polar Vortex of Winter 2020: Links to Record-Breaking Arctic Oscillation and Ozone Loss, Journal of Geophysical Research: Atmospheres, 125, e2020JD033 271, https://doi.org/https://doi.org/10.1029/2020JD033271, e2020JD033271 10.1029/2020JD033271, 2020.

Maher, N., McGregor, S., England, M. H., and Gupta, A. S.: Effects of volcanism on tropical variability, Geophysical Research Letters, 42, 6024–6033, https://doi.org/https://doi.org/10.1002/2015GL064751, 2015.

McGregor, S., Khodri, M., Maher, N., Ohba, M., Pausata, F. S. R., and Stevenson, S.: The Effect of Strong Volcanic Eruptions on ENSO, pp. 267–287, https://doi.org/https://doi.org/10.1002/9781119548164.ch12, 2020a.

McGregor, S., Khodri, M., Maher, N., Ohba, M., Pausata, F. S. R., and Stevenson, S. L.: The Effect of Strong Volcanic Eruptions on ENSO, in: El Niño–Southern Oscillation in a Changing Climate, edited by McPhaden, M. J., Santoso, A., and Cai, W., Geophysical Monograph Series, pp. 267–287, John Wiley & Sons, https://doi.org/10.1002/9781119548164.ch12, 2020b.

Ohba, M., Shiogama, H., Yokohata, T., and Watanabe, M.: Impact of strong tropical volcanic eruptions on ENSO simulated in a coupled GCM, Journal of Climate, 26, 5169–5182, 2013.

Orme, L. C., Ludlow, F., Langton, N., Sjöström, J. K., Kylander, M. E., Murphy, C., Pyne-O'Donnell, S. D. F., Turner, J. N., Li, N., Davies, S. J., Mitchell, F. J. G., and Matthews, J. A.: Storminess in North West Europe and volcanic activity during the Holocene, Climate of the Past, 22, 287–313, https://doi.org/10.5194/cp-22-287-2026, 2026.

Ortega, P., Lehner, F., Swingedouw, D., Masson-Delmotte, V., Raible, C. C., Casado, M., and Yiou, P.: A model-tested North Atlantic Oscillation reconstruction for the past millennium, 523, 71–74, https://doi.org/10.1038/nature14518, 2015.

Paik, S., Min, S.-K., Son, S.-W., Lim, E.-P., McGregor, S., An, S.-I., Kug, J.-S., and Yeh, S.-W.: Impact of volcanic eruptions on extratropical atmospheric circulations: review, revisit and future directions, Environmental Research Letters, 18, 063 003, https://doi.org/10.1088/1748-9326/acd5e6, 2023.

Polvani, L. M. and Camargo, S. J.: Scant evidence for a volcanically forced winter warming over Eurasia following the Krakatau eruption of August 1883, Atmos. Chem. Phys., 20, 13 687–13 700, https://doi.org/10.5194/acp-20-13687-2020, 2020.

Polvani, L. M., Banerjee, A., and Schmidt, A.: Northern Hemisphere continental winter warming following the 1991 Mt. Pinatubo Eruption: Reconciling models and observations, Atmos. Chem. Phys., 19, 6351–6366, https://doi.org/10.5194/acp-19-6351-2019, 2019.

Predybaylo, E., Stenchikov, G., Wittenberg, A. T., and Osipov, S.: El Niño/Southern Oscillation response to low-latitude volcanic eruptions depends on ocean pre-conditions and eruption timing, Communications Earth & Environment, 1, 12, 2020.

Qin, Z., Wang, T., Gao, Y., and Fu, Y.: MPI-ESM Grand Ensemble-Simulated Influence of the Mount Pinatubo Volcanic Eruption on Winter Climate Over the Mid-to High-Latitude Northern Hemisphere Continents, International Journal of Climatology, 45, e8719, 2025.

Robock, A. and Mao, J.: Winter warming from large volcanic eruptions, Geophys. Res. Lett., 19, 2405–2408, https://doi.org/10.1029/92GL02627, 1992.

Robock, A. and Mao, J.: The volcanic signal in surface temperature observations, J. Climate, 8, 1086–1103, https://doi.org/10.1175/1520-0442(1995)008<1086:TVSIST>2.0.CO;2, 1995.

Rohde, R. A. and Hausfather, Z.: The Berkeley Earth land/ocean temperature record, Earth System Science Data, 12, 3469–3479, 2020.

Scaife, A. A. and Smith, D.: A signal-to-noise paradox in climate science, npj Climate and Atmospheric Science, 1, 28, 2018.

Sjolte, J., Adolphi, F., Guðlaugsdòttir, H., and Muscheler, R.: Major differences in regional climate impact between high- and low-latitude volcanic eruptions, 48, e2020GL092 017, https://doi.org/10.1029/2020GL092017, 2021.

https://doi.org/10.5194/egusphere-2026-3738
Preprint. Discussion started: 24 July 2026

Smith, D. M., Gillett, N. P., Simpson, I. R., Athanasiadis, P. J., Baehr, J., Bethke, I., Bilge, T. A., Bonnet, R., Boucher, O., Findell, K. L., et al.: Attribution of multi-annual to decadal changes in the climate system: The Large Ensemble Single Forcing Model Intercomparison Project (LESFMIP), Frontiers in Climate, 4, 955 414, 2022.

Sobel, A. H. and Bretherton, C. S.: Modeling Tropical Precipitation in a Single Column, Journal of Climate, 13, 4378 – 4392, https://doi.org/10.1175/1520-0442(2000)013<4378:MTPIAS>2.0.CO;2, 2000.

Tejedor, E., Polvani, L. M., Steiger, N. J., Vuille, M., and Smerdon, J. E.: No Evidence of Winter Warming in Eurasia Following Large, Low-Latitude Volcanic Eruptions during the Last Millennium, Journal of Climate, 37, 5653 – 5673, https://doi.org/10.1175/JCLI-D-23-0625.1, 2024.

Thomas, M. A., Giorgetta, M. A., Timmreck, C., Graf, H.-F., and Stenchikov, G.: Simulation of the climate impact of Mt. Pinatubo eruption using ECHAM5 – Part II: Sensitivity to the phase of the QBO and ENSO, Atmos. Chem. Phys., 9, 3001–3009, https://doi.org/10.5194/acp-9-3001-2009, 2009a.

Thomas, M. A., Timmreck, C., Giorgetta, M. A., Graf, H.-F., and Stenchikov, G.: Simulation of the climate impact of Mt. Pinatubo eruption using ECHAM5 – Part I: Sensitivity to the modes of atmospheric circulation and boundary conditions, Atmos. Chem. Phys., 9, 757–769, https://doi.org/10.5194/acp-9-757-2009, 2009b.

Toohey, M., Krüger, K., Bittner, M., Timmreck, C., and Schmidt, H.: The impact of volcanic aerosol on the Northern Hemisphere stratospheric polar vortex: Mechanisms and sensitivity to forcing structure, Atmos. Chem. Phys., 14, 13 063–13 079, https://doi.org/10.5194/acp-14-13063-2014, 2014.

Ward, B., Pausata, F. S., and Maher, N.: The sensitivity of the El Niño–Southern Oscillation to volcanic aerosol spatial distribution in the MPI grand ensemble, Earth System Dynamics, 12, 975–996, 2021.

Weber, L., Krüger, K., and Fiedler, S.: On CMIP6 Model Consensus for the Climate Response in Eurasian Winter to Historical Volcanic Eruptions, Geophysical Research Letters, 53, e2025GL120 522, https://doi.org/https://doi.org/10.1029/2025GL120522, e2025GL120522 2025GL120522, 2026.

Weierbach, H., LeGrande, A. N., and Tsigaridis, K.: The impact of ENSO and NAO initial conditions and anomalies on the modeled response to Pinatubo-sized volcanic forcing, Atmospheric Chemistry and Physics, 23, 15 491–15 505, https://doi.org/10.5194/acp-23-15491-2023, 2023.

Wunderlich, F. and Mitchell, D. M.: Revisiting the observed surface climate response to large volcanic eruptions, Atmos. Chem. Phys., 17, 485–499, https://doi.org/10.5194/acp-17-485-2017, 2017.

Yanai, M., Esbensen, S., and Chu, J.-H.: Determination of Bulk Properties of Tropical Cloud Clusters from Large-Scale Heat and Moisture Budgets, Journal of the Atmospheric Sciences, 30, 611–627, https://doi.org/10.1175/1520-0469(1973)030<0611:DOBPOT>2.0.CO;2, 1973.

Zambri, B. and Robock, A.: Winter warming and summer monsoon reduction after volcanic eruptions in Coupled Model Intercomparison Project 5 (CMIP5) simulations, Geophys. Res. Lett., 43, 10 920–10 928, https://doi.org/10.1002/2016GL070460, 2016.

Zhu, F., Emile-Geay, J., Anchukaitis, K. J., Hakim, G. J., Wittenberg, A. T., Morales, M. S., Toohey, M., and King, J.: A re-appraisal of the ENSO response to volcanism with paleoclimate data assimilation, Nat. Commun., 13, 747, https://doi.org/10.1038/s41467-022-28210-1, 2022.